Chemical Vapor Deposition of Cerium Oxide Using the Precursors [Ce(hfac)$_3$(glyme)]

Kimberly D. Pollard, Hilary A. Jenkins, and Richard J. Puddephatt*

Department of Chemistry, University of Western Ontario, London, Ontario, N6A 5B7

Received July 20, 1999. Revised Manuscript Received November 30, 1999

Precursors of formula [Ce(hfac)$_3${MeO(CH$_2$CH$_2$O)$_n$Me}], **1** (n = 1), **2** (n = 2), and **3** (n = 3), and [{Ce(hfac)$_3$}$_2${μ-MeO(CH$_2$CH$_2$O)$_4$Me}], **4** (hfac = CF$_3$COCHCOCF$_3$), have been prepared and used as precursors for chemical vapor deposition (CVD) of films of cerium oxides on the substrates Si, Pt, and TiN. Thermal CVD at 450 °C with oxygen as carrier gas gave mixed Ce(III)/Ce(IV) oxides, and the main crystalline component was Ce_4O_7, but with fluoride impurity. The fluoride impurity was not observed if CVD was carried out using moist oxygen as carrier gas or if the as-deposited films were annealed in oxygen. Codeposition with [Y(hfac)$_3${MeO(CH$_2$CH$_2$O)$_2$Me}] gave films of the mixed Ce(IV)Y(III) oxide $Ce_2Y_2O_7$. The depositions of cerium oxides could be enhanced by use of a palladium precursor catalyst [Pd(2-methylallyl)(acetylacetonate)] and could then be carried out at 250 °C, giving films of CeO_2. Under carefully controlled conditions, films of ceria-supported palladium could be prepared by this method. The films were characterized by using X-ray photoelectron spectroscopy, scanning electron microscopy, and X-ray diffraction techniques.

Introduction

Materials containing cerium oxides have useful applications in catalysis,[1] solid oxide fuel cells,[2] and reversible oxygen storage materials for automobile catalysts,[3] as well as optics and photoluminescence.[4] In many applications, such as in cerium-doped copper oxide superconductors[5] or oxygen storage materials,[6] the easy interconversion between oxidation states of cerium in forming Ce_2O_3 or CeO_2 is important. In developing CVD procedures for *f*-element oxides, there are often problems with reproducibility because common precursors may undergo self-association, hydrate formation, and hydrolysis or cleavage of the ligands on storage.[7−12] In particular, several known precursors for cerium oxides have the disadvantage of leaving residue in commercial evaporators and of having poor stability to atmospheric oxygen or water.[8a] The known precursors for cerium oxides include [Ce(thd)$_4$][13,17−19] (where thd = 2,2,6,6-tetramethyl-3,5-heptanedionato), [Ce$_2$(etbd)$_6$(tetraglyme)][14] (where etbd = 1-ethoxy-4,4,4-trifluorobutane-1,3-dionate and tetraglyme = 2,5,8,11,14-pentaoxapentadecane), [Ce(fod)$_4$][15] (where fod = 1,1,1,2,2,3,3-heptafluoro-7,7-dimethyloctane-3,5-dione), [Ce(fdh)$_4$] (where fdh = 6,6,6-trifluoro-2,2-dimethyl-3,5-hexanedione), [Ce(fdh)$_3$(phen)][16,19] (where phen = 1,10-*o*-phenanthroline), NH$_4$[Ce(fdh)$_4$], Na[Ce(fdh)$_4$],[16] [CeO(thd)$_2$], [Ce(hfac)$_4$], [{Ce(fod)$_3$}$_2$(tetraglyme)],[18] and [Ce(thd)$_3$(phen)].[19] The precursors may contain Ce(III) or Ce(IV) centers. A common strategy for synthesis of stable, water-free, volatile precursors is to saturate the metal coordination sphere by using neutral ligands in

(1) (a) Weyrich, P. A.; Trevino, H.; Holderich, W. F.; Sachtler, W. M. H. *Appl. Catal. A: Gen.* **1997**, *163*, 31. (b) Luo, M.-F.; Zhong, J.-J.; Yuan, X.-X.; Zheng, X.-M. *Appl. Catal. A: Gen.* **1997**, *162*, 121.

(2) Park, I.-S.; Kim S.-J.; Lee, B.-H.; Park, S. *Jpn. J. Appl. Phys.* **1997**, *36*, 6426.

(3) Katuta, N.; Morishima, N.; Kotobuki, M.; Iwase, T.; Mizushima, T.; Sato, Y.; Matsuura, S. *Appl. Surf. Sci.* **1997**, *121/122*, 408.

(4) (a) Nakano, F.; Uekura, N.; Nakanishi, Y.; Hatanaka, Y.; Shimaoka, G. *Appl. Surf. Sci.* **1997**, *121/122*, 160. (b) Morshed, A. H.; Moussa, M. E.; Bedair, S. M.; Leonard, R.; Liu, S. X.; El-Masry, N. *Appl. Phys. Lett.* **1997**, *70*, 1647.

(5) Tranquada, J. M.; Heald, S. M.; Moodenbaugh, A. R.; Liang, G.; Croft, M. *Nature* **1989**, *337*, 720.

(6) (a) Su, E. C.; Montreuil, C. N.; Rothschild, W. G. *Appl. Catal.* **1985**, *17*, 75. (b) Herz, R. K. *Ind. Eng. Chem. Prod. Res. Dev.* **1981**, *20*, 451. (c) Yao, H. C.; Yu-Uao, Y. F. *J. Catal.* **1984**, *86*, 254. (d) Cho, B. K.; Shanks, B. H.; Bailey, J. E. *J. Catal.* **1989**, *115*, 486.

(7) (a) Malandrino, G.; Licata, R.; Castelli, F.; Fragala, I. L.; Benelli, C. *Inorg. Chem.* **1995**, *34*, 6233. (b) Bradley, D. C.; Chudzynska, H.; Hursthouse, M. B.; Motevalli, M. *Polyhedron* **1994**, *13*, 7. (c) Drake, S. R.; Lyons, Z.; Otway, D. J.; Slawin, A. M. Z.; Williams, D. J. *J. Chem. Soc., Dalton Trans.* **1993**, 2379.

(8) (a) McAleese, J.; Plakatouras, J. C.; Steele, B. C. H. *Thin Solid Films* **1996**, *286*, 64. (b) Malandrino, G.; Incontro, O.; Castelli, F.; Fragala, I. L.; Benelli, C. *Chem. Mater.* **1996**, *8*, 1292. (c) Baxter, I.; Drake, S. R.; Hursthouse, M. B.; Abdul-Malik, K. M.; McAleese, J.; Otway, D. J.; Plakatouras, J. C. *Inorg. Chem.* **1995**, *34*, 1384.

(9) Darr, J. A.; Mingos, D. M. P. *Polyhedron* **1996**, *15*, 3225.

(10) Drake, S. R.; Hursthouse, M. B.; Abdul-Malik, K. M.; Miller, S. A. S.; Otway, D. J. *Inorg. Chem.* **1993**, *32*, 4464.

(11) (a) Barash, E. H.; Coan, P. S.; Lobkovsky, E. B.; Streib, W. E.; Caulton, K. G. *Inorg. Chem.* **1993**, *32*, 497. (b) Gleizes, A.; Sans-Lenain, S.; Medus, D.; Hovnanian, N.; Miele, P.; Foulon, J.-D. *Inorg. Chim. Acta* **1993**, *209*, 47. (c) Poncelet, O.; Hubert-Pfalzgraf, L. G. *Polyhedron* **1990**, *9*, 1305. (d) Hirata, G. A.; McKittrick, J.; Avalos-Borja, M.; Siqueiros, J. M.; Devlin, D. *Appl. Surf. Sci.* **1997**, *113/114*, 509.

(12) (a) Grigelionis, G.; Kundrotas, P. J.; Tornau, E. E.; Rosengren, A. *Supercond. Sci., Technol.* **1996**, *9*, 927. (b) Turnipseed, S. B.; Barkley, R. M.; Sievers, R. E. *Inorg. Chem.* **1991**, *30*, 1164. (c) Bradley, D. C.; Chudzynska, H.; Hursthouse, M. B.; Motevalli, M. *Polyhedron* **1994**, *13*, 7.

(13) Leskela, M.; Sillanpaa, R.; Niinisto, L.; Tiitta, M. *Acta Chem. Scand.* **1991**, *45*, 1006.

(14) Baxter, I.; Darr, J. A.; Hursthouse, M. B.; Abdul Malik, K. M.; McAleese, J.; Mingos, D. M. P. *Polyhedron* **1998**, *17*, 1329.

(15) Chadwick, D.; McAleese, J.; Senkiw, K.; Steele, B. C. H. *Appl. Surf. Sci.* **1996**, *99*, 417.

(16) Becht, M.; Dahmen, K.-H.; Gramlich, V.; Marteletti, A. *Inorg. Chim. Acta.* **1996**, *248*, 27.

(17) Becht, M.; Morishita, T. *Chem. Vap. Dep.* **1996**, *2*, 191.

(18) McAleese, J.; Darr, J. A.; Steele, B. C. H. *Chem. Vap. Dep.* **1996**, *2*, 244.

(19) Becht, M.; Gerfin, T.; Dahmen, K.-H. *Chem. Mater.* **1993**, *5*, 137.

10.1021/cm990455r CCC: $19.00
Published on Web 02/29/2000

Chart 1. Some Known Glyme Complexes

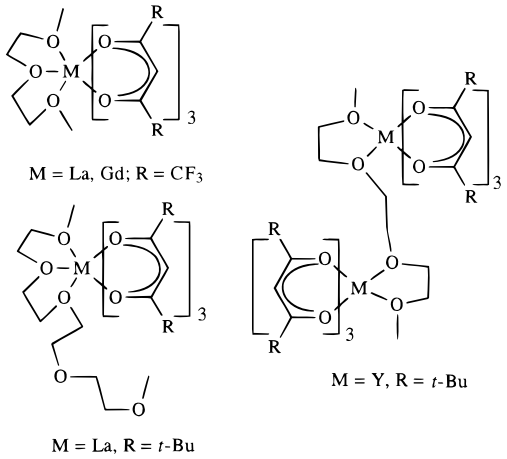

Scheme 1

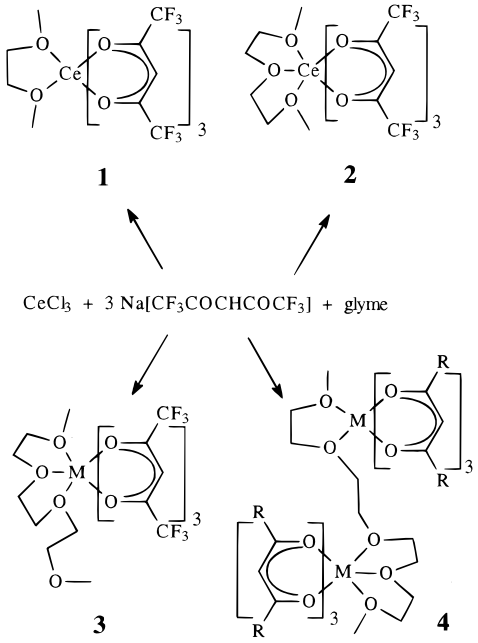

combination with β-diketonate ligands. When the neutral ligand is a glyme {$MeO(CH_2CH_2O)_nMe$, n = 1 (*monoglyme*), 2 (*diglyme*), 3 (*triglyme*), and 4 (*tetraglyme*)}, the complexes may have the structures shown in Chart 1, and examples are known with M = La, Gd, Er, Pr, and Eu.[7−10] This paper describes an extension of this method with the synthesis and characterization of some new complexes [Ce(hfac)$_3$L] {hfac = hexafluoroacetylacetonate, L = *mono−tetraglyme*}, and their properties as precursors in the CVD of cerium oxides and oxide fluorides.

Results and Discussion

Synthesis of Precursors. The complexes, [Ce(hfac)$_3$-{$MeO(CH_2CH_2O)_nMe$}] (n = 1 (**1**), 2 (**2**), and 3 (**3**) and Hhfac = 1,1,1,6,6,6-hexafluoro-2,4-pentanedione), were prepared by reaction of a 1:1 mixture of the appropriate polyether and $CeCl_3$ in benzene with 3 equiv of sodium (1,1,1,6,6,6-hexafluoro-2,4-pentanedionate), [Na(hfac)], according to Scheme 1. They were isolated as air-stable yellow solids. The similar reaction with tetraglyme gave a yellow liquid that was characterized as [{Ce(hfac)$_3$}$_2$-{$MeO(CH_2CH_2O)_4Me$}], **4**. In each case, the complexes could be sublimed or distilled under vacuum without decomposition. The melting points followed the sequence **2** (74−76 °C) > **1** (55−57 °C) > **3** (64−66 °C) > **4** (liquid). Attempts to prepare **1**−**4** by reaction of Ce_2O_3 or CeO_2 with Hhfac and the corresponding polyether were unsuccessful. The structures proposed for **1**−**4** are shown in Scheme 1.

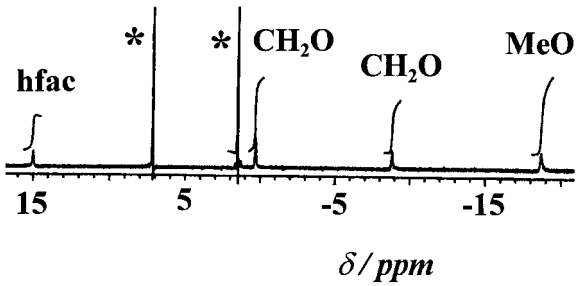

Figure 1. ^{1}H NMR spectrum of **2**, illustrating the unusual chemical shifts arising from paramagnetism. Peaks labeled * are due to protic impurities in the NMR solvent.

Spectroscopic Properties and Fluxionality. The infrared spectra of **1**−**4** contained bands due to the ν(C═O) and ν(C═C) bands of the hfac ligands in the region 1535−1575 cm^{-1}. In addition, bands due to the ν(C−O) stretching modes of the coordinated glyme ligand were present in the range 1097−1060 cm^{-1}, as expected from literature precedents.[20]

The ^{1}H NMR spectra of the complexes show significantly shifted peaks due to the paramagnetic properties of Ce(III), as illustrated for **2** in Figure 1. The ^{1}H, ^{13}C, and ^{19}F NMR spectra of **1**−**3** in dichloromethane-d_2 at room temperature show only one hfac ligand environment (e.g., only one ^{19}F resonance), whereas the eight- or nine-coordinate structures shown in Scheme 1 must have lower symmetry. The spectral data are consistent with a rapid fluxional process occurring at room temperature, leading to exchange of the hfac ligand environments. Because the maximum known coordination number of cerium in complexes such as these is 9, it is likely that at least one of the oxygen atoms in the triglyme ligand of **3** remains uncoordinated (Scheme 1). However, the ^{1}H NMR spectrum of **3** (**[**Ce(hfac)$_3$-(triglyme)**]**) indicates effective symmetry of the triglyme ligand, perhaps indicating easy exchange between eight- and nine-coordinate structures, as indicated in eq 1. At

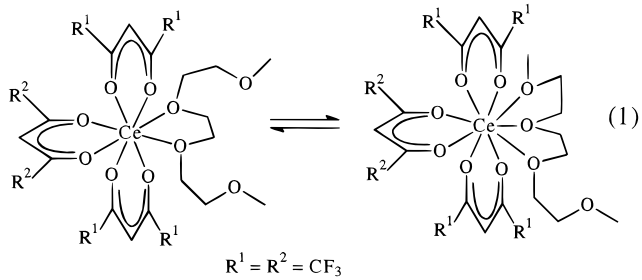

(1)

−60 °C, ^{1}H NMR spectra of **1**−**3** contained very broad peaks, due to complications from the paramagnetism, and they could not be resolved or assigned. The ^{19}F NMR spectra at low temperature were better resolved.

(20) Baxter, I.; Darr, J. A.; Hursthouse, M. B.; Abdul Malik, K. M.; McAleese, J.; Mingos, D. M. *Polyhedron* **1998**, *17*, 1329.

For complexes **1** and **2** at −80 °C, the spectra still contained single ^{19}F resonances, suggesting that the complexes are fluxional even at low temperatures. For **3** at −80 °C, the ^{19}F NMR spectrum resolved to two peaks at $\delta = -70.6$ and −70.3 in a 1:2 intensity ratio. In this case, the fluxionality is partly frozen out at low temperatures. The data do not define the low-temperature structure, but it is likely that the separate ^{19}F resonances are due to the hfac ligands that are roughly trans and cis to the glyme ligand as indicated in eq 1.

The NMR spectra of **4** are more complex than those for **1**−**3**. At room temperature, the ^{1}H NMR spectrum contains very broad peaks due to the protons of the tetraglyme ligand and of the hfac ligands, although the number of peaks still corresponded to the highest possible symmetry (e.g., only one hfac resonance). Integration of the ^{1}H NMR spectrum indicated the stoichiometry shown in Scheme 1. However, the ^{19}F NMR spectrum of **4** at room temperature contained three equal intensity, broad peaks at $\delta = -68.3$, −72.8, and −73.5, indicating nonequivalence of CF_3 groups. Curiously, the ^{13}C NMR spectrum, even at −80 °C, contained only one broad CF_3 resonance, presumably due to accidental degeneracy. The ^{19}F NMR spectrum of **4** at −60 °C contained broad peaks at $\delta = -68.7$, −70.2, −73.1, and −74.2 in a 2:2:1:1 ratio. A possible assignment is shown in eq 2. It is not clear if the solid-

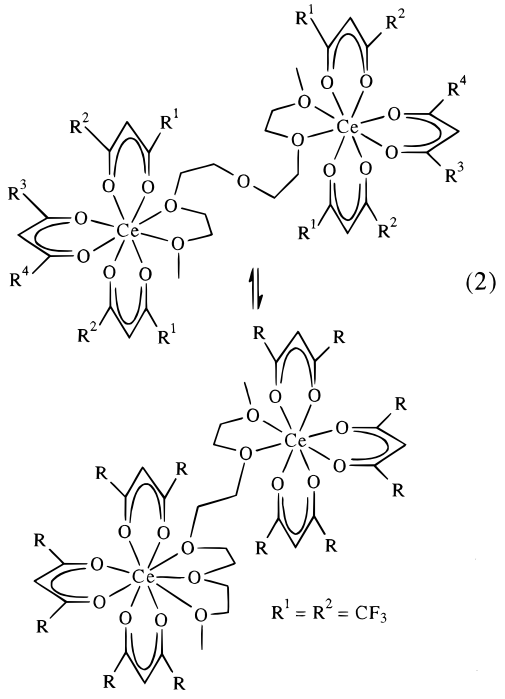

(2)

state structure of **4** contains two eight-coordinate cerium centers or one eight- and one nine-coordinate center (eq 2). The NMR spectra indicate the more symmetrical structure, but this could well be due to very easy fluxionality of the glyme ligand as shown in eq 2. There is precedent for both symmetrical eight-, eight-coordinate and mixed eight- and nine-coordinate structures in related complexes, and the energy difference between them is probably very small.[20,21−23]

The mass spectra of **1**−**4** are summarized in Table 1. Complexes **1**−**3** each give a parent ion, though not of high intensity, but **4** gave only peaks due to complexes

Table 1. Selected Ions in the Mass Spectra of 1−4[a]

fragment	1	2	3	4
$[Ce(L)_3(gl)]^+$	851(5)	895(2)	939(trace)	983(trace)
$[Ce(L)_3]^+$	761(66)	761(23)	761(15)	761(26)
$[Ce(L)_2(gl)]^+$	644(20)	688(100)	732(100)	776(100)
$[Ce(L)_2]^+$	554(72)	554(27)	554(27)	554(28)
$[CeF(L)(C_4HF_3O_2)]^+$	504(81)	504(32)	504(23)	504(32)
$[CeF(L)]^+$	366(100)	366(44)	366(35)	366(15)
$[CeF(C_4HF_3O_2)]^+$	316(58)	316(31)	316(21)	316(10)
$[CeF_2]^+$	178(30)	178(16)	178(18)	178(5)

[a] L = β-diketonate; gl = monoglyme (**1**), diglyme (**2**), triglyme (**3**), and tetraglyme (**4**).

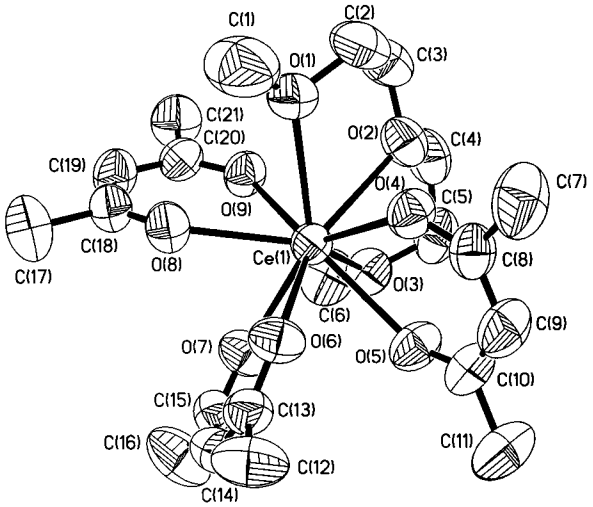

Figure 2. View of the structure of **2**. Hydrogen and fluorine atoms are omitted for clarity.

Table 2. Selected Bond Distances (Å) and Angles (deg) for 2

Ce−O(1)	2.634(4)	Ce−O(6)	2.476(3)
Ce−O(2)	2.621(4)	Ce−O(7)	2.448(4)
Ce−O(3)	2.585(4)	Ce−O(8)	2.485(4)
Ce−O(4)	2.466(3)	Ce−O(9)	2.483(3)
Ce−O(5)	2.493(4)		
O(1)−Ce−O(2)	62.83(13)	O(6)−Ce−O(7)	70.64(12)
O(2)−Ce−O(3)	64.01(13)	O(8)−Ce−O(9)	68.50(12)
O(4)−Ce−O(5)	69.05(12)		

with one cerium atom. In each case, the major fragmentation was due to loss of the glyme ligand, followed by loss of one hfac ligand, or the reverse sequence, to give $[Ce(hfac)_2]^+$ as a major ion.

Structure of [Ce(hfac)$_3$(triglyme)]. A view of the structure of **2** is shown in Figure 2, and selected bond distances and angles are listed in Table 2. The cerium atom in **2** is bonded to the oxygen atoms of three chelating hfac ligands and to all three oxygen atoms of the diglyme ligand, thus giving a distorted nine-coordinate, monocapped, square antiprismatic geometry. The coordination polyhedron around the cerium atom shows considerable distortions from the idealized geometry. The capping atom O(1) lies above the approximately square face defined by O(2), O(4), O(8), and O(9), leaving O(3), O(5), O(6), and O(7) to define the other square face of the square antiprism.

(21) Drake, S. R.; Lyons, A.; Otway, D. J.; Slawin, A. M. Z.; Williams, D. J. *J. Chem. Soc., Dalton Trans.* **1993**, 2379.
(22) Hibbs, D. E.; Darr, J. A.; Hursthouse, M. B.; Malik, K. M. A.; Mingos, D. M. P. *Polyhedron* **1996**, *15*, 3225.
(23) Baxter, I.; Drake, S. R.; Hursthouse, M. B.; Plakatouras, J. C. *Inorg. Chem.* **1995**, *34*, 1384.

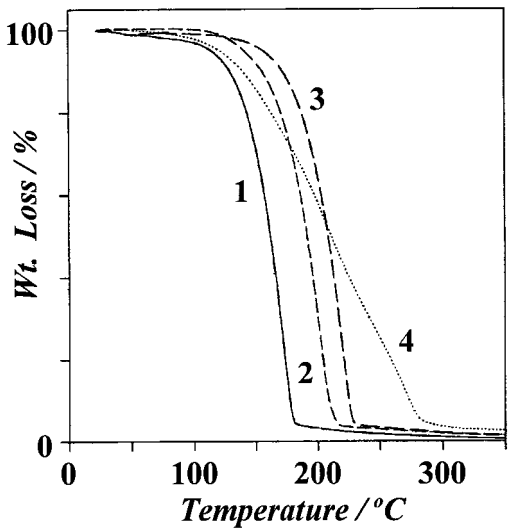

Figure 3. TGA traces for **1**−**4**.

The Ce−O bond lengths associated with the diglyme ligand (Ce−O = 2.585(4)−2.634(4) Å, with a mean of 2.613 Å) are longer than those associated with the β-diketonate ligands (Ce−O = 2.448(4)−2.493(4) Å, with a mean of 2.482 Å). The longest bond corresponds to the bond between cerium and the capping diglyme oxygen atom, O(1). The O−Ce−O chelate angles for the hfac ligands lie in a narrow range, 68.5(1)−70.6(1)°, and those of diglyme in the range 62.8(1)−64.0(1)°, comparable to values in other polyether adducts of lanthanide β-diketonate complexes.[20−23]

Volatility Studies. The complexes **1**−**4** all sublime or distill easily under vacuum, but they also evaporate quantitatively at atmospheric pressure, as shown by thermogravimetric analysis (TGA). The TGA traces are shown in Figure 3. The volatility as measured by the temperature for complete evaporation followed the sequence **1** (ca. 180°) > **3** (ca. 210°) > **2** (ca. 230°) > **4** (ca. 280°). The binuclear complex **4** is the least volatile, although it is a liquid precursor. All are sufficiently volatile to act as good CVD precursors.

Chemical Vapor Deposition (CVD). Films of cerium oxide were grown from the precursors **1**−**4** using a cold-wall, vertical CVD reactor.[24] Thermal CVD was carried out under reduced pressure with the substrate, a fragment of a wafer of TiN(100), Pt(111), or Si(100), heated at 450−600 °C for a period of 2 h. The precursor reservoir was heated to 80−140 °C as needed to give a satisfactory evaporation rate, and the carrier gas was oxygen in most cases, passed at a rate of 100−300 mL min^{-1}. For comparison, some CVD experiments were carried out using moist oxygen, nitrogen, or hydrogen. The resulting films were glossy and mirrorlike and varied in color from very pale red to green. Adhesion to the substrates was good for all three substrates, as determined by tape and scratch tests. Adhesion on silicon is favored by deposition of an oxide on surface silicon oxide and by a good match of the ceria and silicon lattices, and it is noted that ceria, Pt, and TiN all have cubic lattices.

Scanning electron microscopy (SEM) cross-sectional data for ceria films grown on three different substrates at 500 °C with films grown from precursor **3** and using an oxygen carrier gas at a flow rate of 200 mL/min were obtained to determine the relative growth rates of ceria films. The rates of deposition on the substrates Si(100), TiN(100), and Pt(111) were 20, 50, and 95 nm/h, respectively. The film compositions were very similar, but the growth rates were consistently substrate dependent as Pt > TiN > Si.

Table 3. Selected XPS Data for Cerium Oxide Films[a]

precursor substrate	Ce $3d_{5/2}$ BE (eV)	O 1s BE (eV)	anal. Ce	O	C	F
1 TiN	882.5, 888.4 898.2, 886.1	528.9, 531.0	21	68	3	8
2 TiN	882.5, 887.6 899.2, 886.1	528.7, 531.2	17	56	3	14
3 TiN	882.3, 887.7 900.1, 886.2	529.9, 531.2	11	67	5	17
4 TiN	882.6, 887.8 898.8, 886.0	528.9, 531.1	13	70	6	11
1 Si	882.6, 888.0 899.0, 885.8	528.9, 531.8	11	70	1	18
1 Pt	882.8, 887.9 899.0, 886.2	528.7, 531.1	10	84	3	3

[a] BE = binding energy. Relative abundance is recorded in atom percent. All peak binding energies were corrected with respect to amorphous carbon, which was referenced to 285.0 eV. The F(1s) binding energies were 685.0(5) eV in all cases.

Characterization of Films by X-ray Photoelectron Spectroscopy (XPS). Analytical data for films grown at 450 °C using dry oxygen (at a flow rate of 200 mL min^{-1}) as carrier gas are given in Table 3. The films of cerium oxide were characterized by using XPS, following literature precedents.[25−30] There are known difficulties associated with XPS analysis of cerium oxide films using the Ce 3*d* bands, which result from photoreduction during the measurements,[25,26] from complications arising from partial occupation of Ce 4*f* orbitals,[27] and from the tendency of ceria to act as an oxygen storage medium.[28] The cerium 3*d* spectrum of authentic CeO_2 contains three main $3d_{5/2}$ features at 882.6 (u′), 889.3 (u″), and 898.6 eV (u‴) and three main $3d_{3/2}$ features at 900.8 (v′), 907.8 (v″), and 916.7 eV (v‴).[26] The different states arise from the core hole potential in the final state and 4*f* hybridization in the initial state.[26] The Ce 3*d* region in Ce_2O_3 gives two sets of doublets with the $3d_{5/2}$ peak contributions at 880.9 and 885.3 eV and the related $3d_{3/2}$ contributions at 899.7

(24) Yuan, Z.; Dryden, N. H.; Vittal, J. J.; Puddephatt, R. J. *Chem. Mater.* **1995**, *7*, 1696.

(25) El-Fallah, J.; Hilaire, L.; Romeo, M.; Le Normand, F. *J. Electron Spectrosc. Relat. Phenom.* **1995**, *73*, 89.

(26) (a) Paparazzo, E. *Surf. Sci.* **1990**, *234*, L253. (b) Paparazzo, E.; Ingo, G. M.; Zacchetti, N. *J. Vac. Sci. Technol. A* **1991**, *9*, 1416. (c) Park, P. W.; Ledford, J. S. *Langmuir* **1996**, *12*, 1794. (d) Bak, K.; Hilaire, L. *Appl. Surf. Sci.* **1993**, *70/71*, 191.

(27) Creaser, D. A.; Harrison, P. G.; Morris, M. A.; Wolfindale, B. A. *Catal. Lett.* **1994**, *23*, 13.

(28) Trovarelli, A. In *Catalytic Properties of Ceria and CeO_2−Containing Materials*; Marcel Dekker: Germany, 1996.

(29) (a) Purdy, A. P.; Berry, A. D.; Holm, T. R.; Fatemi, M.; Gaskill, D. K. *Inorg. Chem.* **1989**, *28*, 2799. (b) Zhao, J.; Dahmen, K.-H.; Marcy, H. O.; Tonge, L. M.; Marks, T. J.; Wessels, B. M.; Kannewurf, C. R. *Appl. Phys. Lett.* **1989**, *53*, 1750. (c) Larkin, D. L.; Interrante, L. V.; Bose, A. *J. Mater. Res.* **1990**, *5*, 2706. (d) Lingg, L. J.; Berry, A. S.; Purdy, A. P.; Ewing, K. J. *Thin Solid Films* **1992**, *209*, 9.

(30) (a) Girolami, G. S.; Jeffries, P. M.; Dubois, L. H. *J. Am. Chem. Soc.* **1993**, *115*, 1015. (b) Watson, I. M.; Atwood, M. P.; Cardwell, D. A.; Cumberbatch, T. J. *J. Mater. Chem.* **1994**, *4*, 1393. (c) Duray, S. J.; Buckholz, D. B.; Song, S. N.; Richeson, D. S.; Ketterson, J. B.; Marks T. J.; Chang, R. P. H. *Appl. Phys. Lett.* **1991**, *59*, 1503.

Table 4. O:F Ratios for CVD on Some Substrates with Dry or Moist Oxygen Carrier Gas

precursor	Si(100)	TiN(100)	Pt(111)
1[a]	1:0.19	1:0.11	1:0.01
1[b]	1:0	1:0	1:0
2[a]	1:0.29	1:0.22	1:0.02
2[b]	1:0	1:0	1:0
3[a]	1:0.25	1:0.20	1:0.02
3[b]	1:0	1:0	1:0
4[a]	1:0.16	1:0.09	1:0.03
4[b]	1:0	1:0	1:0

[a] Dry or [b]moist carrier gas was used.

and 903.8 eV, respectively; so, there is partial overlap with the peaks due to CeO_2.[26] The O 1*s* spectra of CeO_2 consist of two peak bands, one at 528.8 eV due to oxygen in CeO_2 and one at 531.2 eV due to a hydroxide species,[26] whereas Ce_2O_3 gives one peak at 530.0 eV.[26] The Ce 3*d* spectra reported in Table 3 indicate that the films contain both Ce(IV) (binding energy (BE) = ca. 882, 888, and 898 eV) and Ce(III) (BE = ca. 886 eV). In all cases, the oxygen content of the films was higher than expected for the formula CeO_2 as a result of oxygen storage by the ceria.[28]

The films contained 1−6% carbon impurity, and the carbon impurity was greatest for **3** and **4**, which contained the higher glyme ligands (Table 3). The films contained from 3 to 22% fluorine impurity (Table 3), clearly arising by fluoride abstraction from the hfac ligands.[29] In this case, there was a substrate dependence, with the fluoride impurity level following the series Si > TiN > Pt (Table 3). The fluoride impurity was effectively absent if the CVD experiments were carried out using oxygen carrier gas presaturated with water vapor (Table 4).[30] These fluorine-free films also contained much lower cerium(III) content compared to films containing fluoride, as deduced from the lower intensity of the Ce(III) 3*d* peak (BE = ca. 886 eV) relative to the Ce(IV) peaks (BE = ca. 882, 888, 898 eV). The role of water is to facilitate removal of fluoride from the forming films as volatile HF, and the data indicate that the fluoride is mostly associated with cerium(III) centers.[29,30] The fluorine could also be removed from the impure films by annealing in moist air at 600 °C for 2 h to give pure CeO_2 films, consistent with earlier reports.[31]

Similar CVD experiments were carried out using either hydrogen or nitrogen as carrier gas with the precursor **2**, [(diglyme)Ce(hfac)$_3$] and the substrate Si(100) at 500 °C. The film formed in each case was cerium oxide, but the fluoride impurity level was higher with nitrogen or hydrogen than in CVD using oxygen carrier gas. In addition, the excess oxygen content observed using oxygen carrier gas was much lower when using hydrogen or nitrogen, as would be expected. Overall, there are no advantages to using hydrogen or nitrogen as carrier gas, and moist oxygen is better than dry oxygen in forming films of fluoride-free cerium oxide from precursors **1**−**4**.

Catalysis of Film Formation: CECVD. Introduction of a palladium precursor catalyst has been shown to either decrease the substrate temperature required for deposition of an oxide film or lower the carbon contamination in metallic films.[32] A study of this catalytic effect was reported for CVD of yttria from the precursor [Y(thd)$_3$], thd = 2,2,6,6-tetramethyl-3,5-heptanedionate, and the catalyst complex [Pd(2-methylallyl)(acac)], where acac = 2,4-pentanedionate.[32] It was found that the addition of the catalyst lowered the minimum substrate temperature by approximately 200 °C for thermal CVD to produce Y_2O_3 films, and the effect was termed catalyst-enhanced chemical vapor deposition (CECVD).[32]

Table 5. Selected XPS Data from Palladium-Catalyzed CVD Reactions of Cerium Oxide[a]

CVD process	Ce 3$d_{5/2}$ BE (eV)	O 1*s* BE (eV)	Ce:O:F ratio	substrate
noncatal.	882.4, 887.5, 898.8, 885.4	529.9, 532.2	1:4.6:0.9	TiN(100)
catal.	882.5, 887.2, 898.3, 885.3	529.9, 531.3	1:4.0:0	TiN(100)
noncatal.	882.3, 886.9, 898.6, 885.7	529.9, 532.1	1:5.2:1.1	Si(100)
catal.	882.4, 888.0, 898.6, 885.6	530.0, 531.5	1:6.4:0.2	Si(100)
noncatal.	882.4, 887.6, 898.5, 885.9	529.9, 531.5	1:8.2:0.7	Pt(111)
catal.	882.5, 887.9, 898.9, 886.0	530.0, 532.4	1:5.4:0	Pt(111)

[a] All binding energies are corrected with respect to amorphous carbon at a binding energy of 285.0 eV. Carbon contamination was less than 8%. All XPS values were obtained after 2 min of sputtering with Ar gas excited to 4 keV.

In the present work, catalysis of the formation of ceria films was examined. In initial experiments to compare the compositions of films formed with and without the catalyst precursor, the cerium precursor was transported using the carrier gas oxygen at a flow rate of 200 mL/min and the substrate was heated to 450 °C. Films were deposited with and without the introduction of a catalyst precursor [Pd(2-methylallyl)(acac)], which was introduced into the CVD chamber using a nitrogen carrier gas. The films were analyzed by XPS, and selected data are given in Table 5. The XPS results indicate that cerium is present in both the +3 and +4 oxidation states in each case. However, carbon contamination was reduced and fluorine contamination was eliminated in the films grown by catalyst-enhanced CVD (Table 5).

To test the catalytic effect on the growth rate of ceria, films were grown using precursors **3** and **4** on each of the substrates Si, TiN, and Pt at 250 °C, with oxygen carrier gas at 250 mL min^{-1}, and the palladium catalyst, [(2-methylallyl)Pd(acac)], carried to the reactor by nitrogen at a flow of 15 mL min^{-1}. In all cases, the growth rates obtained by cross-sectional imaging using SEM were in the range 420−490 nm h^{-1}, with no significant trends observed as a function of either ceria precursor or substrate (Table 6). In the absence of the catalyst, there was insignificant CVD under these conditions. The catalytic effect of the palladium precursor is therefore obvious. The use of oxygen carrier gas was important because the catalytic effect was not observed when nitrogen carrier gas was used at the substrate temperature of 250−300 °C. In addition, prior seeding of the

(31) Becht, M.; Gerfin, T.; Dahmen, K.-H. *Chem. Mater.* **1993**, *5*, 137.

(32) (a) Zhang, Y.; Puddephatt, R. J. *Chem. Mater.* **1999**, *11*, 148. (b) Zhang, Y.; Choi, S. W.-K.; Puddephatt, R. J. *J. Am. Chem. Soc.* **1997**, *119*, 9295.

Table 6. Deposition Conditions[a] and Film Composition for Cerium Oxide Films

		film composition[d]		
source materials[b]	*T* (°C)[c]	Ce $3d_{5/2}$ BE (eV)	O 1*s* BE (eV)	growth rate (nm/h)
3/**5**[e]/Si(100)	250/100/23	882.6, 887.5, 898.5, 885.7	529.0, 531.0	425
3/**5**/TiN(100)	250/100/23	882.2, 888.3, 898.2, 885.4	528.6, 531.6	480
3/**5**/Pt(111)	250/100/23	883.0, 888.6, 898.4, 886.4	529.0, 531.9	490
4/**5**/Si(100)	250/100/23	882.7, 888.0, 898.7, 886.0	528.7, 531.2	450
4/**5**/TiN(100)	250/100/23	882.4, 888.0, 898.7, 885.5	528.7, 531.6	425
4/**5**/Pt(111)	250/100/23	882.7, 887.6, 898.4, 885.9	528.6, 531.3	460

[a] In all cases, carrier gas is O_2 at 250 mL/min, pressure is 1 Torr, and Pd content is undetectably low. [b] Precursor/catalyst/substrate. [c] Minimum substrate temperature for film formation/temperature for precursor reservoir/temperature for catalyst reservoir. [d] Analytical values obtained after 2 min of sputtering. [e] **5** is [(2-methylallyl)Pd(acac)].

substrate surface with palladium followed by thermal CVD of cerium oxide under the same conditions as those used in CECVD did not give good films; the co-deposition is clearly important. The films grown by CECVD showed good adhesion in all cases, and the SEM images showed the formation of uniform films with open amorphous structures. The particle sizes ranged from 30 to 80 nm depending on the substrate used. One such image of a catalytically grown film of cerium oxide, grown with precursor **3** on Si(100) at 300 °C with oxygen carrier gas at a flow of 250 mL/min is shown in Figure 4.

The catalytic effect was also studied in similar CVD reactions with nitrogen and hydrogen as the carrier gases. In these cases, cerium oxide was still formed, although the ratio of cerium to oxygen was dramatically reduced and the amount of fluorine incorporation increased significantly. Some results are reported in Table 7 for CECVD experiments using the precursor **3** on Si(100) heated to 450 °C. It was observed that the amount of Ce(III) relative to Ce(IV), as determined from the Ce $3d_{5/2}$ XPS, increased slightly when N_2 carrier gas was used and increased dramatically when H_2 carrier gas was used. This can be understood in terms of film formation in the presence of an oxidizing (O_2), a nonreactive (N_2), or a reducing atmosphere (H_2). As the reducing nature of the atmosphere increased, there was a corresponding increase in fluoride impurity in the film and a decrease in oxygen content (Table 7). These results are similar to those found in the CECVD of yttria/yttrium fluoride.[32] Clearly, the use of oxygen carrier gas is advantageous for the formation of ceria films by CECVD. As discussed previously,[32] it is likely that the true catalyst in these CECVD reactions is palladium metal, present as very small crystallites, and so the palladium complex used is both a CVD and a catalyst precursor, rather than a true catalyst.

Formation of Ceria-Supported Palladium Films. Over the past several years, cerium dioxide and CeO_2-containing materials have come under intense scrutiny as catalysts and as structural and electronic promoters of heterogeneous catalytic reactions, especially as key components in three-way catalysts for the treatment of exhaust gas from automobiles.[33] CeO_2 has been used extensively as a support for metals in heterogeneous catalysis reactions.[33] The traditional role of the support was to disperse and stabilize small metal particles; however, in addition to these effects, several other interactions can also occur at the metal−oxide interface, resulting in substantial modifications of the physicochemical and catalytic properties of both the oxide and the metal. Stabilization of dispersed palladium metal as well as the formation of Pd−Ce alloys under reductive conditions has been attributed to the palladium−oxide interactions.[34] Under oxidative conditions, the interactions between palladium and cerium dioxide are less clear.[28] In this regard, it would be interesting to study bimetallic films of ceria and palladium.

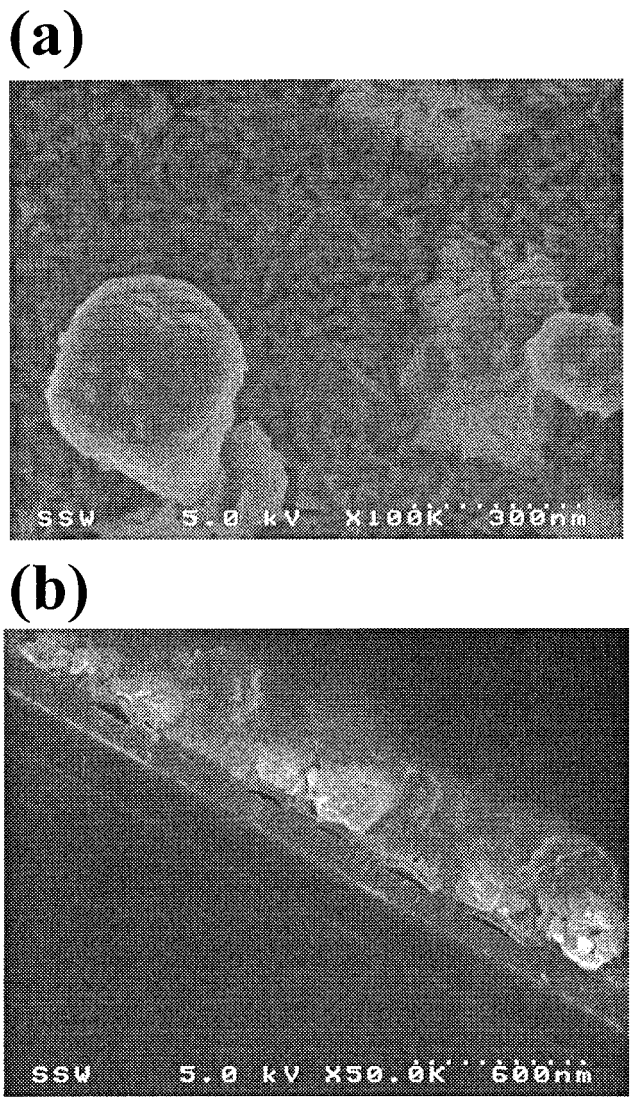

Figure 4. SEM images of ceria films grown from precursor **3** by CECVD at 300 °C in the presence of [Pd(2-methylallyl)(acac)]: (a) top view and (b) cross section.

(33) (a) Summers, J. C.; Ausen, S. A. *J. Catal.* **1979**, *58*, 131. (b) Kim, G. *Ind. Eng. Chem. Prod. Res. Dev.* **1982**, *21*, 267.

(34) Kepinski, L.; Wolcyrz, M.; Okal, J. *J. Chem. Soc., Faraday Trans.* **1995**, *91*, 507.

Table 7. Effect of Carrier Gas on Catalyzed CVD Reactions[a]

carrier gas	Ce 3$d_{5/2}$ BE (eV)	Ce(III):Ce(IV) ratio	O 1*s* BE (eV)	F 1*s* BE (eV)	Ce:O:F ratio
O_2	882.3, 888.3, 898.6, 885.6	0.3:1	528.6, 531.0	N/A	1:7.2:0
N_2	882.1, 888.0, 898.3, 885.2	0.5:1	528.3, 530.9	685.3	1:5.0:0.5
H_2	882.0, 887.9, 898.0, 885.1	2:1	528.0, 530.8	685.0	1:2.8:0.8

[a] All peaks were referenced to amorphous carbon at a binding energy of 285.0 eV.

Table 8. XPS Analysis of Bimetallic Palladium/Ceria Films

prec./subst./subst. temp. (°C)	Ce 3*d* BE (eV)	Pd 3*d* BE (eV)	O 1*s* BE (eV)	Ce:Pd:O ratio	carbon content (atom %)
3/TiN(100)/400	882.5, 888.3, 898.7	335.4	528.9, 531.3	1:1.2:4.3	0
3/Si(100)/400	882.3, 888.5, 898.4	335.6	529.2, 531.0	1:1.3:5.1	8
3/Pt(111)/400	882.7, 889.1, 899.4	335.6	529.3, 531.1	1:1.0:4.6	5

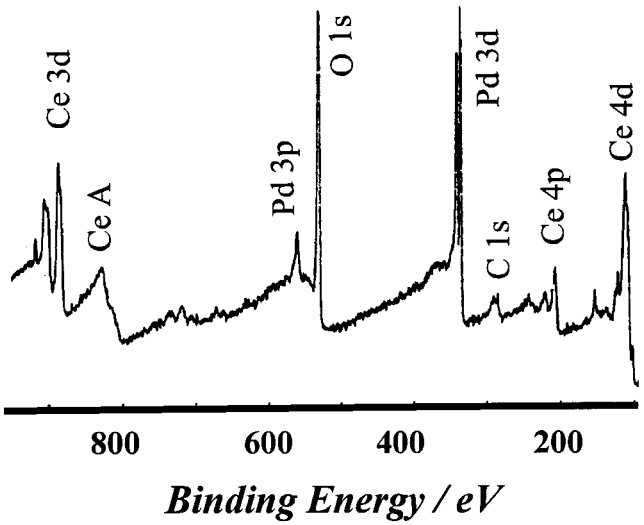

Figure 5. XPS spectrum of a mixed ceria/Pd film.

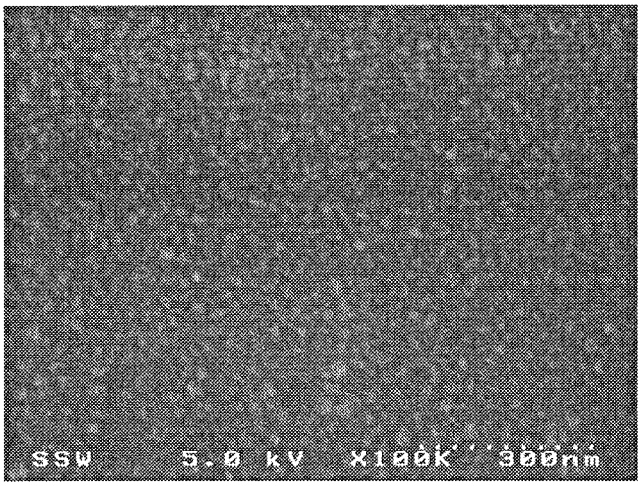

Figure 6. SEM image of a mixed ceria/Pd film. The Pd crystallites are dark, and ceria particles are lighter.

By increasing the amount of palladium precursor flowing into the CVD reaction chamber, bimetallic films can be obtained. These films were difficult to grow because their formation only occurred over a narrow range of conditions. A flow rate of carrier gas oxygen of 200 mL min^{-1} through the precursor **3** at 80 °C and of 25 mL min^{-1} nitrogen through the catalyst precursor [Pd(2-methylallyl)(acac)] at 23 °C, with combination at the substrate at 300 °C was found to give films containing both ceria and palladium, as outlined in Table 8. A typical XPS spectrum of a bimetallic film on a Si(100) substrate is shown in Figure 5.

Palladium is present as palladium(0) as is shown by its binding energy (Pd 3$d_{5/2}$ = 335.6 eV; literature binding energy for Pd metal, 3$d_{5/2}$ = 335.08 eV).[35] The Ce 3*d* region scan in the XPS spectra showed contributions from Ce(IV) only, and so, it is concluded that the cerium is present only as CeO_2.

The films have some carbon contamination (0−8%) but no fluorine incorporation. This would be expected based on the results of the catalytic reactions in which palladium was noticed to decrease the amount of fluorine contamination in the resulting CeO_2 films. The ratio of cerium to oxygen was again much greater than the 1:2 ratio expected, due to oxygen storage.[26]

The bimetallic films are crystalline with particle sizes between 50 and 300 nm. A typical SEM image is shown in Figure 6. EDX analysis shows that the small fine-grained structure (light in color) is ceria, and it is interspersed with palladium crystallites (dark in color).

Cerium/Yttrium Oxide Films and the Nature of Ce(III)/Ce(IV) Oxide. For several potential applications of high-temperature superconductors, it is desirable to deposit films on substrates other than the usual single-crystal materials. In particular, for multichip module designs using $YBa_2Cu_3O_{7-x}$, (YBCO), multilayer structures such as YBCO/YSZ/SiO_2/YSZ/YBCO/CeO_2/YSZ, YSZ = yttria-stabilized zirconia, may be needed.[36] For this study, the last two layers, ceria- and yttria-stabilized zirconia, were of interest, in particular to study whether mixed oxides of ceria/yttria could be formed by CVD.

The films were formed by using a mixture of the precursors [(diglyme)Y(hfac)$_3$] and [(diglyme)Ce(hfac)$_3$] with an oxygen carrier gas at a flow rate of 250 mL/min on TiN(100) heated to 300−400 °C for a period of 2 h. The films were characterized by XPS and XRD (X-ray diffraction) methods. The XRD analysis showed the presence of the crystalline mixed oxide $Ce_2Y_2O_7$ oriented preferentially in the ⟨111⟩ plane (Table 9).[37] XPS analysis showed only Ce(IV) peaks at BE($3d^5/_2$) = 882.4, 887.6, and 898.2 eV and Y(III) peaks at BE($3d^5/_2$) = 158.1 eV, confirming the assignment as Ce(IV)$_2$-Y(III)$_2$O$_7$. XPS analysis also indicated the presence of C(5%) and F(7%) impurities in the film. The nature of

(35) Nyholm, R.; Martensson, M. *J. Phys. C: Solid State Phys.* **1980**, *13*, L279.

(36) Reade, R. P.; Russo, R. E. *Appl. Surf. Sci.* **1996**, *96*−*98*, 726.

(37) *Inorganic Compounds*; Ondik, H. M., Mighell, A. D., Mrose, M. E., Robbins, C. R., Stalick, J. K., Eds.; Crystal Data Determinative Tables, 3rd ed., Vol. 4; U.S. Department of Commerce, National Bureau of Standards and the JCPDS International Centre for Diffraction Data: Swarthmore, PA, 1978.

Table 9. XRD Analysis of $Ce_2Y_2O_7$ and Ce_4O_7[a]

d (Å)	I/I_0 (expected)	I/I_0 (observed)	*hkl*
	$Ce_2Y_2O_7$		
3.100	100	100	111
2.690	60	26	002
1.899	80	35	022
1.619	80	22	113
	Ce_4O_7		
3.10	100	100	111
2.69	60	22	002
1.90	80	33	022
1.62	80	20	113

[a] Expected values are from JCPDS reference no. 9-286 for $Ce_2Y_2O_7$.

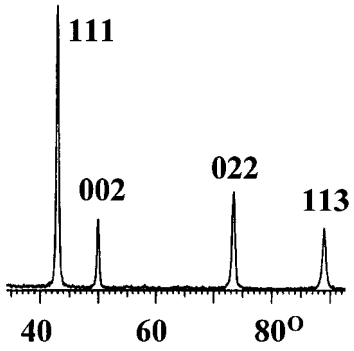

Figure 7. XRD (Cr X-ray source) of Ce_4O_7.

the mixed oxidation state cerium(III)/cerium(IV) oxide phases prepared by CVD was deduced by comparison with the above data. The morphology of a typical film grown from **3** on a silicon dioxide substrate at 450 °C with oxygen carrier gas at a flow rate of 200 mL/min has fine texturing with grains of approximately 40 nm, indicating that growth occurs under conditions of high nucleation but low crystal growth rate. The XRD data showed peaks that were inconsistent with either Ce(III) or Ce(IV) oxide but that were essentially identical with those of $Y_2Ce_2O_7$ (Figure 7 Table 9), although XPS confirmed the absence of yttrium. This indicates that the crystalline oxide phase formed under these conditions is $Ce(IV)_2Ce(III)_2O_7$ or Ce_4O_7, isomorphous with $Ce(IV)_2Y(III)_2O_7$. Because the Ce(III)/Ce(IV) ratio varies in different samples, it is likely that other oxides are present but do not give well-defined XRD peaks. Once again, the strong reflection in the ⟨111⟩ plane is indicative of preferential orientation of the Ce_4O_7 in that direction.[37]

Mechanistic Studies. The mechanisms of CVD of oxides from diketonate complexes are only partly understood, and the mechanisms by which fluoride incorporation occurs from fluorinated complexes are particularly puzzling because the fluorine atoms are at least four bonds removed from the metal in the precursor complexes.[29,38] In this work, exhaust gases from the CVD reactions using precursors [Ce(hfac)$_3$(glyme)] were collected in a liquid-nitrogen-cooled trap and then analyzed by GC/MS techniques. The gaseous products included CO and CO_2/H_2O, which are presumably formed by oxidation of hfac or glyme ligands. The liquid exhaust products show the presence of the glyme ligand and protonated Hhfac ligand. Several minor products were formed but most could not be identified by GC-MS; these all contained a peak at $m/z = 69$, corresponding to the CF_3 group, indicating that they arise by fragmentation of the hfac ligands. One component was identified as $CF_3C(O)CH{=}CF_2$ and, considering that CO is also formed, might occur as shown in Scheme 2.

Scheme 2. Possible Mechanism for Fluoride Formation

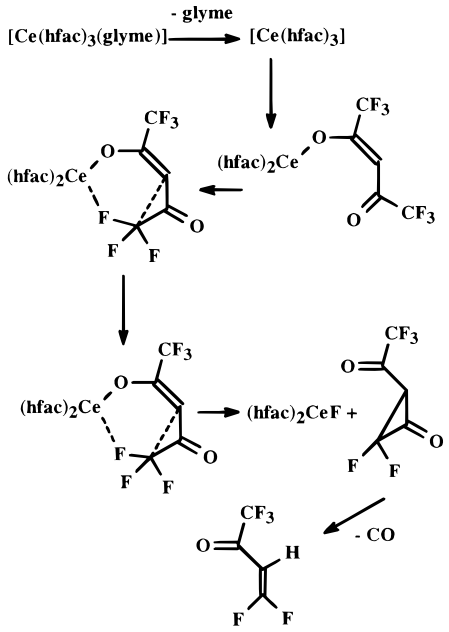

A similar set of experiments was carried out using a palladium-catalyzed CVD reaction, with oxygen carrier gas, and the exhaust products were trapped and analyzed as above. The gaseous products seen were CO_2 and H_2O with no CO detected. The liquid portion indicated the presence of both glyme and Hhfac. Again, many minor products were formed that could not be identified by GC-MS. The results suggest that much decomposition of the cerium precursors occurs away from the palladium catalyst but that the CO is eliminated at the catalyst center and is then oxidized to CO_2.

The observed products of CVD are related to those formed by fragmentation of the precursors in the mass spectrometer (Table 1). The primary step in fragmentation in MS was formation of the $[Ce(hfac)_2]^+$ fragment, by loss of the glyme ligand and one β-diketonate ligand. Subsequent fragmentation leads to formation of fluoride complexes and CO among other products. Several other studies of cerium and lanthanide β-diketonate complexes have also shown that easy fluoride abstraction from CF_3 groups of hfac ligands can occur easily, during fragmentation in the mass spectrometer.[39]

Conclusions

This work describes the characterization of some new solid Ce(III) precursors and one liquid Ce(III) precursor for CVD of cerium(IV) oxide. The complexes are para-

(38) (a) Bradley, D. C. *Chem. Rev.* **1989**, *89*, 1317. (b) Schildcrout, S. M. *Inorg. Chem.* **1985**, *24*, 760.

(39) (a) Dras, M.; Livingstone, S. E. *Aust. J. Chem.* **1975**, *28*, 1513. (b) Livingstone, S. E.; Zimmerman, W. A. *Aust. J. Chem.* **1976**, *29*, 1845. (c) Allcock, M. G.; Belcher, R.; Majer, J. R.; Perry, R. *Anal. Chem.* **1970**, *42*, 776. (d) Das, M. J. *Inorg. Nucl. Chem.* **1981**, *43*, 3412. (e) Morris, M. L.; Koob, R. D. *Inorg. Chem.* **1981**, *20*, 2737. (f) Morris, M. L.; Koob, R. D. *Org. Mass Spectrom.* **1982**, *17*, 503.

magnetic, but NMR studies are useful in studying their stoichiometry and lability in solution. The solid-state structure of **2** was determined and illustrates the preferred geometry of such nine-coordinate complexes. These results contribute to the understanding of the factors that influence volatility in these complexes, which is so important in the CVD process.

Fluorinated complexes increase the volatility of the precursor but still have the disadvantage of contaminating the deposited films with fluorine. In the case of cerium oxide, annealing the film in oxygen at 600 °C for an hour is a successful and very effective way of removing fluoride, and the fluorinated precursors are then shown to be viable for the formation of cerium oxide. Promotion of film formation using a palladium catalyst can be used to enhance the formation of cerium oxides even at temperatures as low as 250 °C. The same cerium(III) precursors can be used to prepare mixed oxide films such as $Ce_2Y_2O_7$ or to prepare mixed oxide−metal metal films such as ceria/Pd, that might have useful catalytic properties.

Experimental Section

^{1}H, ^{13}C, and ^{19}F NMR spectra were obtained in deuterated acetone or dichloromethane by using a Varian Gemini 300 spectrometer. ^{1}H and ^{13}C chemical shifts were referenced to TMS and fluorine chemical shifts to $CFCl_3$. Infrared spectra were measured using a Perkin-Elmer System 2000 FT-IR spectrometer and NaCl pellets. Mass spectra were recorded using a Finnigan MAT 8200 MSS data system. The thermogravimetric analysis was run using a Perkin-Elmer thermogravimetric analyzer TGA7. X-ray photoelectron spectroscopic (XPS) data were recorded on the SSL SSX-100 small-spot XPS surface-analysis instrument with a monochromatized Mg Kα X-ray source (1253.6 eV). The surface composition in atom percent from XPS spectra was collected after 1−2 min of sputtering with argon at 4 keV until a constant composition was given. Top or cross-sectional views of the films were shown using an ISL DS-130 scanning electron microscope. Gas chromatographic-mass spectrometric (GC-MS) studies were carried out using a Varian 3400 gas chromatograph equipped with a DB5 column and a Finnigan MAT 8200 MSS data system. X-ray diffraction patterns were collected at Queen's University on a 12 kW Rigaku Rotaflex model RV-200B with a chromium rotating anode and a Rigaku goniometer with a thin film attachment.

Synthesis and Characterization of Precursors. By following a method similar to that reported previously,[8c] the reaction of $CeCl_3$ with $Na^+[hfac]^-$ and the appropriate polyether in benzene was carried out.

***1**, [(Monoglyme)Ce(hfac)$_3$].* $CeCl_3$ (0.5 g, 1.34×10^{-3} mol.) and glyme (0.14 mL, 1.34×10^{-3} mol) were suspended in benzene and then heated to 90 °C. Hhfac (0.57 mL, 1.33×10^{-2} mol), neutralized with an equimolar amount of NaOH, was added directly into the solution, and the mixture was refluxed for 12 h. While the solution was still warm, unreacted $CeCl_3$ was filtered off. The volume of the solution was reduced to yield a light yellow powder. Recrystallization was carried out in hexane giving a yellow crystalline compound in 82% yield. Mp: 55−57 °C. The complex sublimed quantitatively over the temperature range of 48−60 °C (0.02 mmHg) to give the same product, as determined by its melting point and NMR data. NMR (300 MHz, d_6-acetone): $\delta(^1H) = -18.7$ [s, 6H, OCH_3], −8.9 [s, 4H, OCH_2], 15.0 [s, 3H, CH of hfac]; $\delta(^{13}C) =$ 28.0 [s, OCH_3], 48.0 [s, CH_2], 115.4 [s, CH], 133.8 [q, $^1J_{C-F} =$ 185 Hz, CF_3], 200.3 [q, $^2J_{C-F} = 33$ Hz, CO]; $\delta(^{19}F) = -74.7$ [s]. Anal. Calcd for $CeC_{19}H_{13}F_{18}O_8$: C, 26.80; H, 1.54. Found: C, 26.55; H, 1.70%. MS Calcd for [Ce(hfac)$_3$(glyme)] = 851: Found: 761 (M−glyme)$^+$; 692 (M-glyme-CF_3)$^+$; 644 (M-hfac)$^+$; 554 (Ce(hfac)$_2$)$^+$; 504 (Ce(hfac)$_2$-CF_2)$^+$; 366 (M-glyme-CF_2-CF_3-COCHCO)$^+$; 316 (M-glyme-CF_2-CF_3COCHCO−CF_2)$^+$; 178 (CeF_2)$^+$; 133 ($CH_3OCH_2CH_2OCH_2CH_2OCH_2$)$^+$; 69 ($CF_3$)$^+$.

***2**, [(Diglyme)Ce(hfac)$_3$].* This was prepared similarly from $CeCl_3$ (0.5 g, 1.34×10^{-3} mol.), diglyme (0.192 mL, 1.34×10^{-3} mol), and Hhfac (0.57 mL, 1.33×10^{-2} mol). The yellow crystalline complex product was recrystallized from hexane in 78% yield. Mp: 74−76 °C. The complex sublimed quantitatively over the temperature range 60−75 °C (0.02 mmHg) without decomposition. NMR (d_6-acetone): $\delta(^1H) = -17.6$ [s, 6H, OCH_3], −7.9 [m, 4H, OCH_2], 0.5 [m, 4H, OCH_2], 15.0 [s, 3H, CH]; $\delta(^{13}C) = 31.0$ [s, OCH_3], 44.5 [s, OCH_2], 54.5 [s, OCH_2], 114.5 [s, CH], 118.6 [q, $^1J_{C-F} = 285$ Hz, CF_3], 177.7 [q, $^2J_{C-F} = 34$ Hz, CO]; $\delta(^{19}F) = -74.7$ (s). Anal. Calcd for $C_{21}H_{17}CeF_{18}O_9$: C, 27.20; H, 1.85. Found: C, 28.10; H, 1.89%. MS Calcd for [Ce(hfac)$_3$(diglyme)]: 895. Found: 761 (M−diglyme)$^+$; 688 (M−hfac)$^+$; 554 (M−hfac−diglyme)$^+$ or (M-diglyme−hfac)$^+$, 504 (Ce(hfac)$_2$−CF_2)$^+$; 366 (Ce(hfac)$_2$−CF_2–CF_3COCH)$^+$; 316 (Ce(hfac)$_2$−CF_2−CF_3COCHCO−CF_2)$^+$; 216 (Ce(hfac)$_2$−CF_2−CF_3COCHCO−CF_2−COCHCOCF)$^+$; 178(CeF_2)$^+$; 69 (CF_3)$^+$.

***3**, [(Triglyme)Ce(hfac)$_3$].* This was prepared similarly from $CeCl_3$ (0.5 g, 1.34×10^{-3} mol), triglyme (0.242 mL, 1.34×10^{-3} mol) and Hhfac (0.57 mL, 1.33×10^{-2} mol). The product was a light yellow crystalline compound, which was crystallized from toluene in 74% yield. Mp: 64−66 °C. It sublimed at 55−66 °C (0.02 mmHg). NMR (d_6-acetone): $\delta(^1H) = -9.5$ [s, 6H, OCH_3], −7.2 [m, 4H, OCH_2], −7.4 [s, 4H, OCH_2], −1.2 [m, 4H, OCH_2], 15.0 [s, 3H, CH]; $\delta(^{13}C) = 39.0$ [s, OCH_3], 48.6 [s, OCH_2], 50.0 [s, OCH_2], 56.0 [s, OCH_2], 111.2 [s, CH], 132.0 [q, $^1J_{C-F} = 282$ Hz, CF_3], 197.0 [q, $^2J_{C-F} = 31$ Hz, CO]; $\delta(^{19}F) = -74.8$ (s). Anal. Calcd for $C_{23}H_{21}CeF_{18}O_{10}$: C, 29.30; H, 2.24. Found: C, 28.78; H, 2.28%. MS Calcd for [Ce(hfac)$_3$triglyme)]: 939. Found: 761 (M−triglyme)$^+$; 732 (M−hfac)$^+$; 554 (M−triglyme−hfac)$^+$; 504 (Ce(hfac)$_2$−CF_2)$^+$; 366 (Ce(hfac)$_2$−CF_2−CF_3COCHCO)$^+$; 316 (Ce(hfac)$_2$−CF_2−CF_3COCHCO−CF_2)$^+$; 178 (CeF_2)$^+$; 133 ($CH_3OCH_2CH_2OCH_2CH_2OCH_2$)$^+$; 103 ($CH_3OCH_2CH_2OCH_2CH_2$)$^+$; 69(10.4) ($CF_3$)$^+$.

***4**, [(Tetraglyme){Ce(hfac)$_3$}$_2$].* This was prepared similarly from $CeCl_3$ (0.5 g, 1.34×10^{-3} mol), tetraglyme (0.295 mL, 1.34×10^{-3} mol), and Hhfac (0.57 mL, 1.33×10^{-2} mol) and was isolated as a yellow liquid. The complex distilled intact at 50−68 °C (0.02 mmHg). NMR (d_6-acetone): $\delta(^1H) = -9.6$ [s, 6H, OCH_3], −2.2 [m, 4H, OCH_2], −1.6 [s, 4H, OCH_2], −0.9 [s, 4H, OCH_2], −0.3 [s, 4H, OCH_2], 14.1 [s, 6H, CH]; $\delta(^{13}C) = 50.6$ [s, OCH_3], 58.6 [s, OCH_2], 60.1 [s, OCH_2], 61.1 [s, OCH_2], 62.7 [s, OCH_2], 112.1 [s, CH], 131.8 [q, $^1J_{C-F} = 258$ Hz, CF_3], 195.2 [q, $^2J_{C-F} = 31$ Hz, CO]; $\delta(^{19}F) = -69.8$ (s), −73.7 (s), −74.9 (s). MS Calcd for [Ce(hfac)$_3$tetraglyme)]: 983. Found: 776 (M−hfac)$^+$; 761 (M−tetraglyme)$^+$; 692 (M−tetraglyme−CF_3)$^+$; 554 (Ce(hfac)$_2$)$^+$; 504 (Ce(hfac)$_2$−CF_2)$^+$; 366 (Ce(hfac)$_2$−CF_2−CF_3COCHCO)$^+$; 316 (Ce(hfac)$_2$−CF_2−CF_3COCHCO−CF_2)$^+$; 178 (CeF_2)$^+$; 133 ($C_6H_{13}O_3$)$^+$; 69 (CF_3)$^+$.

Collection and Reduction of X-ray Data. Crystals of [(diglyme)Ce(hfac)$_3$], **2**, were grown from a saturated hexane solution. A crystal was mounted on a glass fiber, and data were collected using a Siemens P4 diffractometer using XSCANS software.[40] Crystal data and refinement parameters for [(diglyme)Ce(hfac)$_3$] are listed in Table 10, and selected interatomic distances and angles are listed in Table 2. Unit cell parameters were calculated from 25 centered high-angle reflections in the range $15 < 2\theta < 25$. Systematic absences indicated the space group $P2_1/n$, and this was borne out by successful refinement of the structure. Semiempirical absorption corrections based on psi-scan data were applied, and full-matrix least-squares refinement of F^2 was performed using SHELXTL version 5.03.[79] All non-hydrogen atoms were refined with anisotropic thermal parameters, including the fluorine atoms, which were somewhat disordered, but no constraints were necessary. The largest residual electron density peak (0.535 eÅ^{-3}) was associated with the cerium atom. In the final stages of refinement, $R_1 = 3.96\%$ and $wR_2 = 9.77\%$.

Metal Organic Chemical Vapor Deposition. A cold-wall vertical Pyrex CVD reactor, fitted with two carrier gas inlets,

(40) *SHELXTL Software*, version 5.03; Seimens Analytical X-ray Instruments Inc.: Madison, WI, 1994.

Table 10. Crystal Data and Refinement Parameters for [(Diglyme)Ce(hfac)$_3$], 2

empirical formula	$C_{21}H_{17}CeF_{18}O_9$
crystal system, space group	monoclinic, $P2_1/n$
unit cell dimensions	$a = 10.350(2)$, $b = 15.919(3)$, $c = 19.787(4)$ Å, $\beta = 96.80(1)°$
temperature (K)	294(2)
volume/Z	3237(1) Å^3/4
D_{calc}	1.837 g/cm^3
radiation type, wavelength	Mo−Kα X-rays (0.710 73 Å)
absorption coefficient (corrected)	1.553 mm^{-1} (Ψ-scan techniques)
diffractometer type (method)	Siemens P4 diffractometer ($\omega/2\theta$)
structure refinement	SHELXTL ver. 5.03 (Sheldrick 1994)
reflections measured	7238 [5697 with $I > 2\sigma(I)$]
observations/parameters	5279/524
R_1/wR_2 [$I > 2\sigma(I)$]	0.0396/0.0977
R_1/wR_2 (all data)	0.0610/0.1122
goodness-of-fit on F^2	0.929

was used for all depositions. The substrate was cleaned by washing in acetone and distilled water and was then mounted horizontally, using silver paint, and was heated by using a rod heater. Approximately 0.25 g or 0.5 mL of the precursor was deposited in the precursor reservoir at the base of the reactor, the whole system was evacuated (1×10^{-3} mbar), and the substrate heater was turned on and left to reach thermal equilibrium. The precursor reservoir was then heated, and the carrier gas was added. CVD reactions were carried out over 2 h time intervals. For catalyst-enhanced CVD, the catalyst complex, [(2-methylallyl)Pd(acac)], was transported to the reaction chamber with nitrogen carrier gas from a separate precursor reservoir. Because of the high volatility of the palladium complex, no heating was required. The ceria precursor was held in the reservoir at the base of the reactor and typically transported using oxygen carrier gas. The two carrier gases were mixed close to the heated substrate where CECVD occurred. Substrates were 1 cm × 1 cm fragments cut from 100-oriented TiN, 100-orientated Si, and 111-oriented Pt wafers.

Acknowledgment. We thank the NSERC (Canada) and MMO for financial support.

Supporting Information Available: Tables of X-ray data for **3**. This material available free of charge on the Internet at http://www.acs.pubs.org.

CM990455R